

Interactive interpretation of 3D surfaces in field-based geosciences using mobile devices - concepts, challenges and applications

Melanie Kröhnert^{a,*}, Christian Kehl^e, Sophie Viseur^b, Simon J. Buckley^{c,d}

^a*Institute for Photogrammetry & Remote Sensing, TU Dresden, Helmholtzstr. 10, 01069 Dresden, Germany*

^b*Aix Marseille Université, CNRS, IRD, CEREGE UM 34, Dept. Sedimentary and Reservoir Systems, 13001 Marseille, France*

^c*Uni Research AS – CIPR, Nygårdsgaten 112, 5008 Bergen, Norway*

^d*Department of Earth Science, University of Bergen, Allégaten 41, 5007 Bergen, Norway*

^e*Danmarks Tekniske Universitet, DTU Compute, Richard Petersens Plads, Building 321/208, 2800 Kongens Lyngby, Denmark*

Abstract

Keywords: discrete geometry, surface reconstruction, volume reconstruction, surface parameterization, digital outcrops

2010 MSC: 00-01, 99-00

1. Introduction

A considerable number of domains within the geosciences rely on digitised natural observations and their interpretation to steer and constrain numerical models. Published (semi-)automatic interpretation methods emerged within the past decade that support the digital documentation of observations and interpretations. These advanced interpretation techniques require increasingly complex computing that is restricted to office-based work environments, which poses a problem for field-based studies. Domains such as hydrology, geology or glaciology hence established multi-stage procedures where observations are taken manually in the field and later digitised in the office. This is disadvantageous

*Corresponding author

Email addresses: melanie.kroehnert@tu-dresden.de (Melanie Kröhnert), chke@dtu.dk (Christian Kehl), viseur@cerege.fr (Sophie Viseur), Simon.Buckley@uni.no (Simon J. Buckley)

and within the referred domains, there is an increasing desire to facilitate digital interpretations in the field at the study location. Mobile computing equipment (e.g. smartphones and tablets) are one technological option to facilitate such digital field-based workflows. These devices are nowadays ubiquitous and can
15 easily be equipped in field-based research. Also, as seen in technical magazines and the general media, the range of available devices continuously increases, which allows to find a "fit-for-purpose" device to each specific situation. New application cases, which are demonstrated and discussed in this article, and commitment within geoscience- and computer technology industry lead to an
20 increasing interest in this cross-disciplinary domain between mobile computing and geoscientific interpretation.

Next to easily available, pocket-format computing devices, the required three-dimensional base data for modern applications also need to be available and being processed in a "mobile-ready" manner. The availability of topographic 3D surface data is steadily increasing due to easy-to-use software and instrumentation for surface generation (e.g. drones, structure from motion (SfM)
25 [1] and multi-view geometry [2], satellite digital elevation models (DEMs)). Furthermore, crowdsourced data and Volunteered Geographic Information (VGI) contribute to the geoscience data inventory, which is acquired by citizen scientists.
30

Domain-specific mobile software is required in order allow for data interaction on the available mobile devices. Specific challenges such as power consumption, multi-manufacturer support, smart sensor utilisation and device intercommunication distinguish mobile software from common desktop software. This
35 leads to a very different design electronics design of tablets and smartphones in comparison to desktop PCs and laptops, which in turn means that existing approaches for digital data processing and interpretation are not transferable as-is to this new computing domain. Even when considering the fast technological development, there are some challenges within mobile device software
40 development that are rooted in the technology itself: user interfaces need to be specifically designed for mobile devices so to utilise touch screen interfaces, nat-

ural language interfaces and gesture interaction (e.g. "swipe" and "optical lens" motions). global navigation satellite system (GNSS)-based geo-localisation accuracy, as delivered by the integrated-circuit sensor of mobile, is inferior to
45 common user expectations and requirements in geoscientific studies. The modalities of sensor data delivery (be it hardware sensor or software emulation), photo capturing and processing, and the computational capabilities of mobile devices differ significantly between each vendors. Short-comings such as inappropriate data structuring, visual object correlation and registration, increasing
50 data volumes and the unavailability of off-the-shelf program codes further complicate the technological development. Addressing the demonstrated challenges distinguishes the mobile application development and common desktop software development for geoscience purposes. **the same as in line 34?**

This article demonstrates how the above-listed challenges can be addressed
55 to provide, in the end, the desired added value for field-based research. This demonstration addresses the 3D data annotation and interpretation for two use cases within the domains of surface hydrology and (petroleum) geology. The content covered in the article is a detail-driven extension of earlier published research [3], focussing on extensive measurements to verify the reasoning and
60 statements of previous studies.

The sections within this article adhere to the following structure: First, the use cases are presented as opening statements to introduce field-related tasks that are to be addressed with mobile device technology. Secondly, different 3D surface data representations are introduced that employed within this technical
65 research. Thirdly, algorithmic baseline concepts that are key for interpreting 3D data on mobile devices are introduced, summarising project-internal development by the authors as well as referencing key literature on the subject. Fourth, the algorithms are mapped to the specific mobile technologies and components. The technologies and major parameters that impact the target use case application are highlighted. Finally, we showcase and discuss how available mobile
70 systems are used in application scenarios from hydrology and petroleum geology to improve data analysis and integrate outdoor measurements in digital

workflows. Then, the article is finalized with some concluding remarks and a discussion for future developments in this research trajectory.

75 **2. Target case studies**

TO-BE-FILLED

3. Representation basis – Geometry and Radiometry

Various representation forms for 3D terrain data are available. While early digital systems used gridded DEMs for their simplicity and compact storage [4, 5], digital surface models (DSMs) and triangulated irregular networks (TINs) are dominating most terrain-based systems for application-specific analysis [6, 7]. A useful example can be seen in [8] for glaciology, where the authors use a triangulated digital surface model to represent a Patagonian glacier front. For triangular surfaces, it is important to distinguish geometrically valid TINs from polygon soup surfaces. While the latter is often employed in early stages of mesh-based software systems due to its simplicity and ease of implementation, valid TINs are employed in mature stages of the analysis. This is because some automated analysis (e.g. auto-interpretation, volume derivation) require clean surfaces with coherently outward-oriented surface normals.

90 In geoscience domains such as petroleum geology, texture- and color information are vital for interpretation- and analysis tasks. In these cases, as demonstrated by Buckley et. al [6] and Caumon et. al [7], the TIN is supplemented with photographic information that is projected on the surface as textures.

95 [ASK SIMON FOR USAGE OF IMAGES FROM VOG - use own reconstruction of Whitby cliffs for nice TINs]

In other geoscience domains, such as hydrology and free surface flow management, on the one hand georeferenced laser scanner point clouds, and on the other one colored point data streams provided by terrestrial photogrammetry for small- or unmanned aerial vehicle (UAV) for large-scale use cases, both processed by application of SfM, are used for several tasks like coastal monitoring

[9, 10], soil erosion and rain-induced landslide observation or even monitoring river's topography [11]. Nevertheless, new approaches for low-cost and on-the-fly river monitoring [12] and simulation [13] arise due to globally increasing flash flood events after heavy rainfalls [14] that are further addressed in section.

105 Since SfM became state of the art in geosciences, the acquisition of (true-)colored "point cloud" models is not that difficult and commonly employed because of their rapid processing (compared to conventional approaches like terrestrial laser scanning (TLS)). Regarding 3D annotation, nearest neighbour analysis provide an opportunity whereby surface triangulation can be avoided.

110 The stated base concepts of geometric representation and radiometric texture information are also valid for mobile device software. Because of the limited processing speed of mobile chipsets, the usage of point cloud appears most common within the graphics literature (e.g. Garcia et. al [15]). Because the sparse vertex distribution in point clouds causes problems in the data analysis, DEMs 115 have seen a revival in the mobile computing domain. DEMs provide dense, closed geometric models that can be rendered and processed very efficiently. Furthermore, with the inferior memory capacity of mobile devices in comparison to laptops and workstations, the possible compression options for point clouds and DEMs are advantageous. Base mapping applications such as Google 120 Maps use DEMs, derived from light detection and range (lidar) or satellite data [16], as their main topographic data representation. Other systems within the geosciences processing 3D data on mobile devices, such as "Outcrop" and Geological Registration and Interpretation Toolset (GRIT), employ genuine textured triangulated DSM from lidar, drone or SfM sources.

125 The chosen form of model representation significantly impacts the algorithms and analytical capabilities employed on the mobile device. Although all algorithms presented in this article work on either form of representation, some of the algorithms favour the treatment of triangulated surfaces (e.g. image-to-geometry registration, guided interpretation), while others clearly favour point-based representations (e.g. rendering).

4. Algorithms

This section demonstrates novel- as well as existing algorithms and methods on mobile devices that are used for solving analysis tasks in the geoscience use cases laid out in section ??.

¹³⁵ As mentioned before, the effectiveness of each algorithm depends on the applied model representation.

4.1. Image-to-geometry registration

- short description what it does
 - how is it generally employed
 - relation to mobile devices
 - approaches and implementation known on mobile devices
 - integration to the above-mentioned use cases
- ¹⁴⁰

Image-to-geometry algorithms aim register 2D images to a given 3D surface, providing a transformation from 2D coordinate system to 3D coordinate system as follows:

$$P' = \begin{pmatrix} u \\ v \\ w \end{pmatrix} = [R_{3,3}|T_{1,3}] \cdot P \quad (1)$$

$$P = \begin{pmatrix} x \\ y \\ z \end{pmatrix} \quad (2)$$

$$P' \in \mathbb{R}^2 = \frac{P'}{w} \quad (3)$$

¹⁴⁵ Using this coordinate system transformation in combination with a known interior camera orientation, it is possible to project each image on the surface. Specific objects outlined in the image, such as image-based interpretations, can also be mapped on the surface. In the geosciences, these algorithms are employed

to create a direct correlation between 3D model and the screen- or image space
150 on which annotations and interpretations are based on [17].

Amongst the published literature, feature-based registration algorithms are most common. Here, salient points (e.g. SIFT, SURF, Harris corners) or edges within the photograph and rendered image of the target 3D model are used to establish an image-to-image correlation.

155 In order to establish a 2D–3D correlation, there are two prevalent approaches available: for triangle mesh models, the 2D feature locations within the rendered image are raycasted using the virtual camera’s vanishing point, the imaging plane and the 3D surface model (see fig. XYZ in [17]). The intersection between the ray and a triangle within the mesh result in the correlated 3D coordinate of the 2D feature. An alternative approach is needed for point-based models because the raycasting does not apply to point representations (i.e. points cannot be intersected directly due to their zero-extent). The alternative approach often applied (see [? ? ?]) employs smart rendering techniques that virtually expand the point into an area feature (e.g. blob, disk or sphere), which 160 is subsequently rendered into a depth map. Afterwards, the 3D coordinate of a 2D feature can be inferred directly from the depth map. Though cleverly utilising graphics technology, this approach is limited by an accuracy-to-speed trade-off: low-resolution and low-quantisation depth maps introduce artificial accuracy errors in the registration process, whereas high-resolution depth maps 165 (above 512^2 pixels) cost considerable performance in the image generation. This last point is particularly important when employing depth map algorithms on mobile devices.

When 2D–3D point pairs are established, the coordinates are normalized and put into a least-squares optimization system, where the target is to determine
175 the exterior camera parameters $(t_x, t_y, t_z, \psi, \varphi, \theta)$ from the 2D–3D point-based equation system. Non-linear optimisation systems (e.g. Levenberg-Marquardt) are applied to estimate the desired parameter set. The whole process can easily be executed on mobile devices [17]. One of the prevalent practical challenges when employing feature-based image-to-geometry registration is to achieve a

¹⁸⁰ reliable feature correlation, which is often achieved by introducing application-specific constraints (e.g. horizon alignment, straight-edge enforcement or object outlines).

¹⁸⁵ Feature-based registration is the most common approach for establishing image-to-geometry correlation on mobile devices due to its implementation simplicity, its rapid execution speed, its option for application-specific constraints and the wealth of available code that can be used. Examples for the application of the technique are ample within the literature, ranging from augmented reality [18, 19] over field geology [17, 20] to surface hydrology [12, 21]. These mobile apps utilize the open-source library *OpenCV4Android*¹, which is also employed in this work². Problems in real-world cases are posed to this technique from imaging variances, resulting in reduced reliability (i.e. failing to determine any camera parameters) and stability (i.e. determining different parameters for the same sets of images). An completely alternative technique to feature-based methods is Mutual Information (MI) [22, 23]. MI performs a pixel-wise comparison between the photo I_{2D} and the 2D rendering of the 3D scene I'_{3D} and aims at minimizing the image discrepancies (i.e. $\operatorname{argmin}\delta(I_{2D}, I'_{3D})$). The technique uses information theory quantities such as self-information and entropy in order to compare the similarity of both image. In contrast to the challenge of feature correlation, MI faces challenges in the optimization process: the optimization ¹⁹⁰ of a 7 degree-of-freedom equation system ($t_x, t_y, t_z, \psi, \varphi, \theta, f$, for f being the focal length) is unstable and prone to rest in local function minima. Only few optimisation solvers are known that can solve such equation systems reliably and provide stable results - most notably NEWUOA (i.e. Powell's method[24]) ¹⁹⁵ used in [23]. As these stable solvers are not available in modern and mobile-device programming languages, the use of MI is currently prohibited for mobile platforms.

¹OpenCV4Android 2.4.10 - <https://opencv.org/platforms/android/>

²OpenCV4Android extensions at https://github.com/CKehl/opencv4Android_extension

While the task of image-to-geometry registration can be offload to remote computers in the network, it is advantageous to perform the registration on the mobile device itself. This is because, in the overall target of model interpretation, the interaction and actual interpretation (as explained in section ??) is more intuitive for the user when being performed on photos and images. If the registration of the images is done on the mobile device, it allows for direct feedback and ad-hoc visual quality checks of the interpretations on the underlying 3D surface model. Furthermore, as shown by measurements in section ??, it can be argued that 2D interpretation more energy efficient than direct 3D interpretations. Lastly, in settings where network access and offline processing is prohibited, an on-device registration procedure is without alternatives.

4.2. Mesh-based rendering

Rendering a surface model in this context refers to the image generation of the 3D data by projective rasterization to the 2D image plane of a virtual camera. This process is performed on mobile devices for the purpose of model presentation as well as for the generation of a synthetic reference image for image-to-geometry registration. Furthermore, it can be used to synthesize an image from available 3D data for interpretation and annotation in 2D.

Algorithms for rendering textured triangulated surfaces are well-known amongst technology-affine personnel. In the common rendering pipeline, the textured mesh is transferred as a set of (attributed) vertices and primitive sets (e.g. triangles, polygons) to the graphics processing unit (GPU). The virtual camera is set up using the pre-defined view projection matrix while the graphics primitives are repositioned using the model-related transformation matrix. The rasterizer projects the available 3D information into the camera plane and performs hidden-surface removal. The result is a discrete-space pixel representation. Modern programmable shaders allow in-time vertex decompression (see [25]) as well as texture decompression (see section ??). Available textures are mapped as images on the surface using the texture coordinate vertex attributes. The mesh-based rendering algorithms employed on desktop computers are ana-

logous to mobile devices, whereas the technological details are posing the actual challenges.

4.3. A novel approach to mobile point-based rendering

In comparison to mesh-based rendering, simple point projection seems to be a nice alternative saving computational resources and efforts for post-processing concerning outlier removal due to falsely surface reconstruction (e.g. blobs due to critic point normals). Thus, we simply project object points onto image plane using perspective projection with assumption of distortion-free ideal camera with centred principle point. Thus, the camera matrix \mathbf{K} equals identity matrix \mathbf{I} and can be neglected in the following equations that generally base on notations given by Szeliski(2010). First, applying a six-parameter transformation transfers three-dimensional object points from world reference frame \vec{X}_W into a 3D camera system \vec{X}_c using

$$\vec{X}_c = \mathbf{R} (\vec{X}_W - \vec{X}_0) \quad (4)$$

where \mathbf{R} is a 3×3 orthonormal rotation matrix and \vec{X}_0 the translation vector to camera's projection center. For simplicity, the usage of the planar Cartesian UTM system with x pointing to the east and y pointing to the north with respect to the prevalent zone number. For z component, the height over the Earth Gravitational Model 1996 (EGM96) is advisable to use. Counting for homogeneous coordinates, we can describe the relation between camera \vec{X}_c and image coordinates \tilde{x} involving their depth components.

$$\begin{pmatrix} \tilde{u} \\ \tilde{v} \\ c_c \end{pmatrix} = \begin{pmatrix} x_c \\ y_c \\ z_c \end{pmatrix} \quad (5)$$

For image plane we introduce camera constant c_c that defines the distance between camera's sensor and projection center in [mm] and is also known as focal length f . To separate camera sensor system and image system, we use the term c_c when talking about sensor [mm] and f for digital image coordinates [px].

For conversion, c_c must be divided by sensor's pixel pitch. For 3D to 2D projection, homogeneous coordinates must be divided by their depth components resulting in inhomogeneous coordinates.

$$\vec{X}_{Cam} = \begin{pmatrix} \frac{\tilde{u}}{c_c} \\ \frac{\tilde{v}}{c_c} \\ 1 \end{pmatrix} = \begin{pmatrix} \frac{x_c}{z_c} \\ \frac{y_c}{z_c} \\ 1 \end{pmatrix} \quad (6)$$

Thus, two-dimensional coordinates can be described with

$$\begin{pmatrix} \tilde{u} \\ \tilde{v} \end{pmatrix} = \begin{pmatrix} \frac{x_c}{z_c} \cdot c_c \\ \frac{y_c}{z_c} \cdot c_c \end{pmatrix} \quad (7)$$

For a final transformation of 2D sensor coordinates into image pixels, we must shift the origin to left upper corner and scale the coordinates that are still in global units by pixel's relation in meters per pixel p_s . Finally, we derive image coordinates (u, v) for an ideal camera using

$$\begin{pmatrix} u \\ v \end{pmatrix} = \frac{1}{p_s} \begin{pmatrix} \frac{x_c}{z_c} \cdot c_c - u_0 \\ \frac{y_c}{z_c} \cdot c_c - v_0 \end{pmatrix} \quad (8)$$

²⁴⁰ 4.3.1. Calculation of 3D bounding box of interest and image plane

Referring to the described use case of situation-based water level determination using a smartphone-camera based gauge (6.1), we need to define a region of interest regarding 3D point projection to render only user's field of view (figure 1). Thus, bounding box defining points to be projected must be calculated using camera position and orientation from fused smartphone sensors. Thereby it must be noted, that the heading is used for viewing direction only, tilt and roll are excluded. Because of uncertainties regarding exterior information (??), bounding box must be expanded to cover more object space than described by sensors as well as cameras field of view. Because of possible noise due to positioning, constants r and dh describe the domain of projection center's uncertainties parallel to image plane. For errors in depth, we define the correction $c = \frac{r}{\tan(H)}$ for shifting the projection center along camera axis. The box is widened by the horizontal H and vertical V opening angles with a fixed

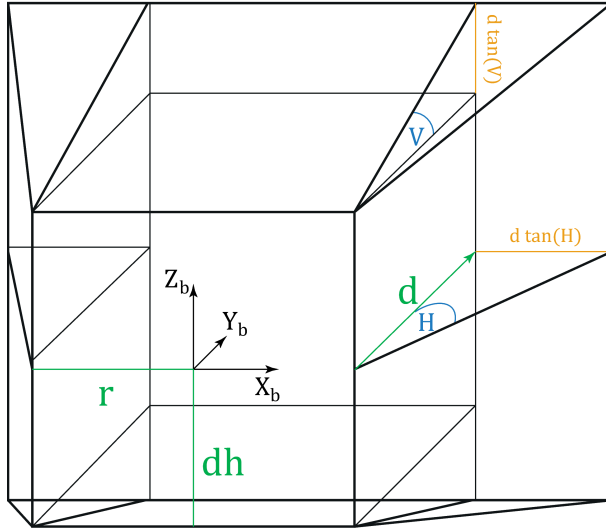


Figure 1: Bounding box definition.

depth d . In order to generate reference data for image-2-geometry intersection to annotate 3D data by mobile imagery, the lateral accuracy given by mobile positioning system as well as the prevalent camera characteristics solve for the mentioned parameters. For camera based gauging, we set $d = 200[m]$. Regarding 3D point projection, each potential point will be checked laying in the box. Therefore, additional tiling of the 3D data set is advisable. Using the defined frustum of a pyramid as region of interest with local reference system, the image plane for 3D point rendering can be defined by perspective projection of the remote xz plane (1) with

$$\vec{X}_b = \begin{pmatrix} -r - d \tan H \\ d \\ dh + d \tan V \end{pmatrix}$$

for bounding box' background plane upper left and

$$\vec{X}_b = \begin{pmatrix} r + d \tan H \\ d \\ -dh - d \tan V \end{pmatrix}$$

lower right corner. Its height equals the height component in world reference frame z_w . Because of pyramid frustum, we finally must eliminate outer points between the smaller front and larger rear plane considering the eight extremes.
[workflow for outer point removal necessary?](#)

²⁴⁵ *4.3.2. Pyramid approach for depth filtering*

Because of a limited range of pixels with defined size inside a image plane it seems to be obvious that in most cases more than one 3D object points corresponds to the same image pixel. Due to inhomogeneous coordinates it is not possible to figure out afterwards which points are in foreground compared
²⁵⁰ to the camera distances and which ones are behind and so not visible. This problem can easily be solved during point cloud projection described above by a simple camera-to-object distance check. However, one problem still remains in case of e.g. glass fronts with lacking information (in TLS due to deflected lidar or SfM when having homogeneous surfaces) or small archs (see figure 3)
²⁵⁵ Then, points might be visible pointing away from camera projection center. On the one hand, point normals may solve the problem but due to data acquisition technique and model's complexity, they are more or less easy to derive ([Sattler zitieren](#)). Remedyng image pyramids are a nice alternative approach used in this case. Therefore, multiple synthetic images are generated with step-by-step
²⁶⁰ adjustment of p_s (see eq. 8), commonly by doubling which resulting in halve numbers of image rows and columns per layer. Than, the algorithm verifies if two pixels corresponds in two subsequent layers, preserving edges (figure 2,3).

4.3.3. Filling gaps due to missing points

Because of pixel size and image plane definition with a specific resolution
²⁶⁵ (that depends in case of 6.1.2 on smartphone camera's resolution) there will be still gaps inbetween projected points (see figure 3, right). To fill these gaps, we recommend to use a simple nearest neighbour approach using binary search [26] in 3D domain to fill these gaps applying weights to average 3D points color attributes depending on their euclidean distances. For this, thresholds for

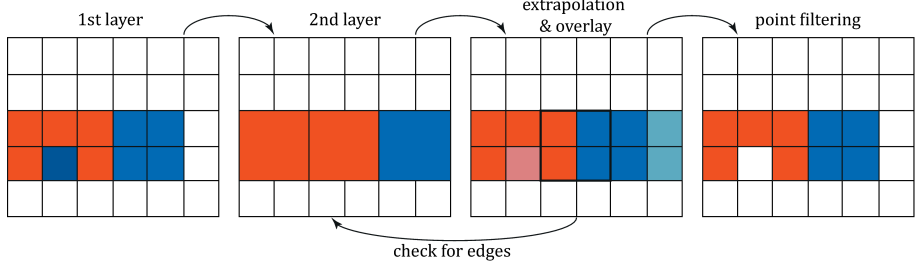


Figure 2: Visualisation of hierarchical depth filtering to handle point occlusions.

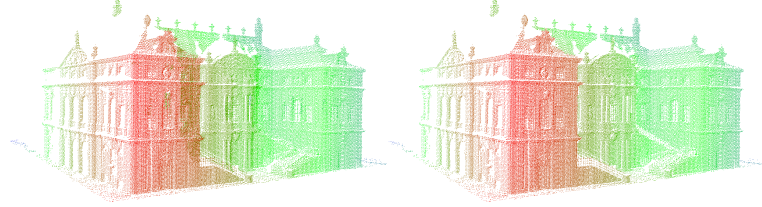


Figure 3: Left, actually obscured visible 3D points close to archs and windows. Right, edge preserving result after filtering.

maximum distances between 3D points must be applied to avoid unreasonable gap-filling. Exemplary for use case 6.1 results before and after gap filling are visualised in figure

4.4. Interpretation and annotation

Interpretation and annotation techniques aim to map geometries (e.g. lines, polygons) of domain-specific information to the 3D base surface. The mapped geometries are used to delineate interest boundaries or to segment the surface into semantically meaningful units.

In hydrological cases, line interpretations are commonly used to mark current water levels as well as high-tide or high-surge water levels. Health monitoring of dykes and levees can use line interpretations to mark cracks within surge defense structures. In geological cases, a mixture of line- and polygon geometries are used. Line interpretations are more commonly related to structural rock features (e.g. cracks, fractures, fault zone boundaries, stratigraphic boundaries),



Figure 4: Fill image gaps using nearest neighbour binary search in 3D domain.

while polygonal area segmentation are more common in sedimentology (e.g. 285 depositional elements, sedimentary objects, sediment facies). That being said, application of the geometries within geology is flexible, as observed in the case of fault facies that use area marks for structural features.

The delineation and mapping can be performed in various ways, depending 290 on the geometric representation of the 3D base surface geometry. Point clouds and 3D TINs can be annotated in directly in 3D. In such application, area markings can be directly embedded as vertex attributes while closest-vertex searches (for point clouds) or view-surface intersections (for TINs) provide the corners for line interpretations. The largest problems with such direct-3D approach on mobile devices are the data size of the underlying surface and complexity of neighbourhood searches. Nearest neighbour search has a computational complexity 295 of $O(nd)$, where $d = 3$ for 3D surfaces and n being the number of vertices in the dataset. This results in non-interactive execution times for 3D vertex marking on mobile devices with real-world datasets (with $n \geq 10^7$). Performing interpretations in 3D on mobile devices also require supportive interaction schemes, 300 including intuitive and easy-access switches between 3D space orientation and actual point selection for the user. Other issues for general direct-3D surface interpretation include the a sparse vertex distribution and open, non-convex geometry (being a particular problem for TINs), surface occlusion and intricate problems related to curved surfaces, where the euclidean vertex distance and

³⁰⁵ geodesic distance along the surface can differ significantly.

Utilising the aforementioned image-to-geometry registration (section ??), the given issues of direct-3D interpretation and 3D interaction can be circumvented. The raster image interpretation is computationally more efficient due to the gridded data arrangement and easier to use for novice practitioners on mobile devices. The interpretation geometries are generated as 2D vector graphics elements, which are projected on the 3D surface after the image registration using the estimated external camera orientation or pose.

5. Technology

5.1. Sensors

³¹⁵ 5.1.1. Localization

- references: ...

5.1.2. Orientation

- stability IMU (see 3D-NO)
- precision IMU

³²⁰ 5.1.3. Parameter sensitivity

5.2. Graphics

PUT SOMEWHERE HERE A REFERENCE TO osgAndroid AS EMPLOYED RENDERING LIBRARY

- as explained above, rendering 3D data is a key part for conducting annotations on 3D data, either based on 3D geometry itself or correlated images in camera space
- for mobile devices, this can technologically be realized two-fold, depending on the usage constraints

- generally, rendering stages (image-place projection, rasterization, tessellation & lighting, see [27]) can be realised by means of software or by hardware support
330
- here, compute operations (gaussian smoothing, derivative computations, vertex projection) are implemented on the mobile device CPU by available operations and libraries using the Android SDK (Java) and Android NDK (C++) on Google's Android system and Swift and Objective-C on Apple's iOS platform
335
- software-based rendering is more flexible in how operations are carried out as they do not need to account for hardware-specific processing pipelines; in the realm of mobile devices, non-standard software-based rendering operations are supported by a wider range of devices
340
- drawback of software-based rendering is performance as it makes suboptimal use newer computing capabilities and graphics-specific chipset operations
345
- example is the novel rendering approach for point-based rendering introduced in section ??, which requires implementation flexibility
- most 3D rendering is done, even on mobile devices, with hardware-based rendering to varying degrees
- even when implementing specific rasterization algorithms (see section ??), operations such as vertex projections and tessellation & lighting are performed on the GPU
350
- hardware-based rendering on mobile devices is facilitated by Khronos' graphics library for embedded systems (GLES) [28] on specialised mobile device graphics chips (e.g. Qualcomm Adreno, ARM Mali, NVIDIA Tegra)
- in comparison to software-based rendering, hardware acceleration provides improved performance
355

- drawbacks of hardware implementations are considerably longer development cycles, because the programming principles of GPUs differ considerably from common "App programming, and reduced flexibility on what can be realised
- ³⁶⁰
- for geoscientists and domain experts in the field, the distinction is good to be aware of as accelerated graphical apps for solving domain-specific tasks are usually offered as paid services to offset the increased development costs
- ³⁶⁵
- external circumstances and project constraints may govern implementation details for graphical systems
 - major constraint imposed in this context is internet availability
 - applications that are expected to operate in an urban setting or in well-developed infrastructure environments can make use of internet access
- ³⁷⁰
- this allows the externalisation of rendering tasks for 3D models and data to a network-oriented client-server architecture as in Ponchio et al. [25]
 - field experts that use apps and require 3D-rendered information can submit rendering requests to a remote server that takes over the image generation of the 3D data
- ³⁷⁵
- technically, the app then only transmits metadata about storage location of the 3D data and receives the final, rasterised image, which allow energy-efficient operability
 - furthermore, the process is agnostic to the specific mobile device generating the request, so this way of implementation works in the exact same manner for all mobile device regardless of the system manufacturer (e.g. Google, Apple, Microsoft)
 - the reduced process load by externalising the rendering tasks allows using advanced algorithms for sensor tracking [] for improved localisation and
- ³⁸⁰

orientation or augmented reality [] for information overlays and multimedia content

385

- in other geoscientific settings, such as field geology [] and environmental monitoring [] of remote areas, internet access is either restricted or expensive to establish

390

- subscription to satellite network with the required data rate costs around 70 euro per month \$ (see www.skydsl.eu, skyDSL2+ flatrate with 30 MBit/s download); data rate needed as high-resolution images with real-time rendering rates (uncompressed 1920x1080 pixels resolution at 30 frames/s amounts to 1.39 GBit/s) requires highest data rates even when employing advanced compression techniques

395

- thus, for geoscience applications that operate in remote areas, web-based rendering is not an option
- in these cases, rendering needs to be done on the device

400

- for on-device rendering, the 3D data need to reside in the device memory and image generation needs to be done with performance-restricted hardware

405

- as is shown in section ??, on-device rendering has considerable impact on the energy consumption

- on-device rendering that processes realistic field data requires considerable implementation efforts, as demonstrated by apps such as OpenWaterLevel [], GRIT [29] and Outcrop [30]

410

- principle scientific advances in mobile device rendering have demonstrated considerable progress over the years [15, 31, 32]

- scaling up smaller laboratory results with mobile graphics to realistic geoscience data, in terms of image quality and resolution as well as 3D base data, is a persisting challenge

- although technical development continuously provides more powerful devices, mobile devices need to sacrifice capabilities such as sensor availability as well as physical size and weight in order to provide larger memory space and higher-performance processors; examples for this trade-off manufacturing can be seen in special-purpose and high-performance tablets such as NVIDIA Shield³, Project Tango resp. ARCore⁴ and Google Pixel C⁵
- an specific problem for geoscientists and domain experts in on-device rendering settings: trade-off between app response time, image quality, hardware utilization and cross-device operability
- in interviews amongst field geologists at the department of earth science at university of Bergen, a major demand from the target user base of such mobile app is interoperability between Android, Microsoft and Apple devices; demand originates from platform-agnostic working of common geoscience software on desktop computers for Apple and Windows
- on the other hand, app responsiveness and high image quality are amongst the next common priorities behind interoperability; user base asks for improved quality when operating advanced equipment (e.g. special-pirpose tablets, novel- and high-performance tablets)
- both demands are conflicting, as making use of specialised hardware (e.g. 64-bit, streaming SIMD extensions (SSE) and vectorisation, parallel processing and GPU Computing such as CUDA⁶ for image processing [33, 34], texture compression [35]) in turn means reducing the range of devices being able to operate the software
- these technologies are key as they provide technical solutions available

³NVIDIA Shield - <https://developer.nvidia.com/develop4shield>

⁴Google Augmented Reality - <https://developers.google.com/ar/>

⁵Google Pixel C- <https://www.android.com/tablets/pixel-c/>

⁶CUDA - <https://developer.nvidia.com/cuda-zone>

right now to achieve the required responsiveness and image quality

5.3. Power consumption

- power consumption is a metric of major importance for mobile field applications

440 • metric governs the operation time of an app outdoors for specific studies; in application domains such as field geology, the target operation time is in the range of four to eight hours without recharging at an electricity plug

445 • for the use cases of waterline detection and field interpretation, we measured the energy consumption of the apps "OpenWaterLevel" and "GRIT" and its relation to technical indicators, such as central processing unit (CPU)- and GPU utilisation, memory consumption and environment measures that influence chip operations, namely the processor temperature

450 • the following measures for both apps were obtained on a Google Nexus 5 smartphone with 4-core ARM Cortex CPU and Qualcomm Adreno GPU; furthermore, OpenWaterLevels and its CPU-related measures were validated on a Samsung S8 smartphone with an 8-core ARM Cortex CPU of newer generation

455 • currently, the only app available on Android that allows measuring metrics on an app-specific level (i.e. logging the power consumption related to just one specific external app) is the Trepn Profiler⁷

460 • while this profiling app runs on all Android devices, the metrics that can be recorded (e.g. GPU load, processor temperature) vary between devices, so that GPU load measurements are not available for the Samsung S8 smartphone

⁷Trepn Profiler -

- also the reason why measurements have been carried out on Google smart-phones instead of other tablets; general insight on processor-power con-sumption behaviour are possible to be extrapolated to other devices
- 465 • in the first test, we compare the power consumption in relation to CPU-and GPU utilisation
- our initial expectation is the a higher GPU load results in an increased power consumption compared to CPU-dominated operations, because mo-bile GPUs draw more power than CPUs to realise the increased graphics performance
- 470 • the results are shown for GRIT during 6.5 minutes of operations in fig. ?? (split in GPU and CPU contribution) and for OpenWaterLevel during 3.5 minutes of operations in fig. ??
- observable in both apps: a clear dependency with CPU load and power consumption; shows that apps enter a state of conservative energy con-sumption if being inactive
- 475 • furthermore, when comparing CPU-dependent and GPU-dependent en-ergy graphs, we observe that peak energy consumption strongly relates to GPU activity
- for measurements in "GRIT", we also have to distinguish between two operation modes
 - actions such as image-to-geometry registration [] and 3D outcrop viewing employ 3D data processing and GPU computations in a major scale, while the image-based interpretation of an outcrop uses 2D image operations within Android-optimized data structures
- 480 • fig. ?? and ?? depict the 2D use case, whereas fig. ?? and ?? show the energy consumption in 3D operations
- 485

- as clearly observable in fig. ?? in comparison to fig. ??, the 3D operations result in a drastic energy cost, raising the average power consumption by XYZ mA
- 490
- in contrast to novice expectation, the CPU load also increases in a 3D data processing setting
 - that is because the CPU of the mobile processor needs to deliver the geometric- and texture data to the GPU; also, the CPU needs to decompress the texture image files, resulting in a higher processing load
- 495
- conclusions from the measurements are manifold
 - on the level of assessing the profiled apps "OpenWaterLevel" for hydrological studies and "GRIT" for field geology studies, we obtained benchmark measures for their power consumption
 - for OpenWaterLevels, the app can be operated with an average of XYZ mA per minute (XYZ mA/h), allowing a theoretical operability on a Google Nexus 5 smartphone of XYZ hours
- 500
- for GRIT, we distinguish between 2D- and 3D operability
 - in 2D operation mode, only conducting image-based interpretations, GRIT consumes XYZ mA per minute (XYZ) per hours, allow XYZ hours of operation
 - on the other hand, if being operated consistently in 3D-mode, the same app consumes XYZ mA per minute (XYZ) per hours, allow only 0.something hours of operation
- 505
- more generally speaking, the study shows that it is important for geoscience users to be aware of the which data they are working with on the mobile device
 - even though 3D may be readily available for a given study, it is not advisable to access them on the mobile device over stretched periods, as the

515 drastically increased power consumption results in an operation time of
XYZ hours with two external power packs in the field bag

- 520
- considering the CPU load behaviour in 3D-mode, we can also hypothesize about the positive impact of utilising hardware-specific operations such as GPU texture decompression on energy consumption: while using the GPU requires generally more power, it is also more efficient in operations such as texture decompression, therefore potentially having a positive affect on the overall power consumption of mobile field apps

6. Applications and Requirements

525 Due to the increasing usability of mobile devices for in the field annotations, several use cases concerning geosciences has become apparent. In the following, two essential

6.1. Derivation of hydrological parameters: Water level gauging

530 The last decade is characterized by a continued increase of globally devastating flash floods after heavy rainfalls. Even smallest creeks turned into hazardous streams causing flooding and landslides. Conventional gauging stations provide precise information about water levels measured over a short time period. State of the art techniques for administrative observation comprise water pressure sensors, floating gauges and conventional tide gauges. They are characterised by long-term stability and outdoor robustness providing accuracies of several millimeters up to one centimeter [36]. Averaged over defined time intervals, it is 535 advisable to remain caution regarding these accuracies may be too optimistic [37] .

540 Because of high costs in purchase and maintenance, gauging stations with complex sensing devices must be sparsely installed. A prime example here is the hydrological network in Saxony, Germany. Here, 184 gauging stations are installed for permanent observation on 154 of 259 rivers rising from small, medium and large catchments [38, 39]. Thus, around a third is not monitored

neither during flood events when the most protection is required. Recently,
commercial smartphone applications arose to enable crowd-sourcing based water
545 level estimation for, among other things, such cases [40, 41]. But all of them have
one thing in common: the water level is entered manually by engaged citizen
scientists finding and photographing tide gauges close to rivers that makes - on
the one hand a potential danger to themselves (f.e. by sudden landslides), and
still limits on the other the approaches to open and visible gauges.

550 Improvements in this sense can be achieved through *image-2-geometry intersection* and 3D annotation for automatic water level determination without
reference gauges for almost every situation regarding running waters. for this,
the smartphone application *Open Water Level* that bases on the freely available
open source camera framework *Open Camera* [42]. Open Water Level allows
555 for free stationing water line detection using short hand held time-lapse image
sequences (for details please refer to [?]). To interpret these, image measure-
ments must be transformed into object space. Thus, exterior information needs
to be provided by smartphone sensors for orientation and positioning.

6.1.1. Requirements applying to the sensors

560 To solve the task of autonomous water level determination on running rivers
f.e. emergency cases using *image-2-geometry intersection*, citizen scientists po-
sition and orientation must be know. As figured out in 5, smartphone sensors
accuracies for orientation and location are highly dependent on user's envi-
ronment. Especially the strong correlation of heading and disturbing magnetic
565 sources may be a issue must be solved specifically related to running rivers where
metal railings usually exists. Similar effects can also be noted using high-end
IMU systems for instance autonomous car navigation. But the magnetic influ-
ences inside cars are almost stable and can be calibrated during the drive (ad-
vanced navigation manual). For smartphone orientation, the magnetic strengths
570 attaching the phone may change substantially in short time. A typical scenario
would be: a citizen scientist walks along street, taking his phone inside the bag-
gage close to metallic keys. While walking he passes several street lamps, signs,

etc. Finally, he arrives at a bridge over a urban river, takes out the phone, looks down to the river and records the time lapse image sequence a few centimetres above a metallic railing. Meanwhile, several cars passing the same bridge. In this simple use case, the magnetic field around the smartphone changes countless times due to several unpredictable disturbances ([table mag disturb](#)) [43].
575
The heading angle has the highest influence compared to pitch and roll regarding 2D image and 3D object data registration. For this, a so-called synthetic image is rendered from colored 3D reference point clouds using scientist's location and orientation to define a situation-dependent bounding box of points to be projected onto image plane with respect to depth and indentations (see [21]). Thereby the heading defines the rotation of the depth direction, as a false angle gives a false viewing direction resulting in a synthetic image that has no similarity or only a little with the time lapse sequence. However, in case of no similarity and thus no possible solution for *image-2-geometry intersection*, simply no water level can be calculated. But in case of slight overlapping, there might be image matches but with very bad distribution that impedes a correct positioning ([fig heading test](#)) and may lead to even worse results of false water levels.
580
585
590

It is obvious that a second source for destructive results exists: the absolute geo-positioning using smartphones currently installed GNSS receivers. In urban scenes with several shadow effects due to high-rise buildings, errors of several meters in latitude and up to more than 30 meters in height are highly possible where even the weather has impact [44, 43, 45]. It is likely that, in the near future, smartphone's GNSS modules will be improved solving lateral accuracies of 50 centimetres [46].
595

For now, possible relief might come including other sources for positioning like digital elevation models for simple height correction or invoke map services that allows the user for position refinement. For this, some APIs are already provided by Google ([quellen](#)) but they are rather cost-expensive by extensive accessing. Another upcoming option is including barometers in sensor fusion, altitude can be measured within three meters [47] but for now, they are not a standard.
600

- 605
- (table, observation heading during water line detection outside → check magnetic strengthens and there changes over short times)
 - (figure/table, sensitivity analysis → heading changed in terms of 10 degrees, what does it make for)

6.1.2. Requirements applying to the scenario

- 610
- *online processing and position refinement: need online connection*
 - *image quality for water line detection: influence of image resolution, lighting, ...)*
 - available approach to address the task

6.2. Field Geology

The goal of geological fieldtrips is to gather insight in the rock record and the structural- and sedimentary rock architecture of a given location. Rock architecture can be studied within subsurface seismic records, but this approach suffers from inferior imaging resolutions and physical limitations of the surveying technique. Therefore, surface outcrops are used for the study. Outcrops can be scanned with modern equipment (e.g. lidar [6, 48], drones [49] and SfM [50]) to generate digital surface representations. The most common representations of digital outcrops are coloured point clouds and textured TINs.

The geological aspect is introduced by interpreting the outcrop models. In this case, interpretations refer to (i) line marks for separating stratigraphic layers, (ii) surface-projected polygons to highlight structural- and sedimentary facies or specific architectural elements and (iii) minor ticks (e.g. lines, points, patterns) to indicate depositional attributes such as deposition orientation or grain geometry. The interpretations were until recently performed in a two-step process: sketches are drawn by hand in the field to document the field geologist's observation of the architecture. After the fieldtrip, the observations are digitalised in the office by transferring the sketched architecture on the available digital outcrop. From there on, further study goals (e.g. geomodelling)

are pursued. As recently published, this workflow is currently being transformed into an integrated digital workflow in the field using mobile devices (see [51] for further details).

635 Geological interpretations can be documented on various scales, but from observations of the author most interpretations are conducted on medium-range. This results in an average observation distance for architectural interpretations of between 100m to 500m to document individual depositional elements and further distances of around 400m to 1400m to document the overall stratigraphic
640 framework of an outcrop. Therefore, as a result of perspective observations, the required lateral localisation accuracy is in the range of $\leq 2.5m$ for the individual element setting and $\leq 8m$ for the wide-angle stratigraphic setting. While achieving the former resolution can still be challenging with mobile sensors (see section ??), the latter resolution is almost guaranteed for GPS localisation. The
645 more important problem is in the vertical resolution: the vertical observation position has, especially in close-distance observations, a drastic impact on the view perspective. Even more important, a vertical localisation error of $\geq 1.5m$ may result in positioning the mobile device "under ground", making any image-based registration impossible. It is this vertical accuracy that is crucial for
650 mobile device interpretation systems to work. Several improvements, such as DEMs and barometric altitude [20], have been proposed to reduce the vertical positioning error while there is still room for novel research proposals to provide more accurate vertical positioning or ground-based constraints on the altitude estimation.

655 One of the dominant challenges for digital field geology is the free availability of 3D surface models. Currently, research groups in the domain (e.g. from the University of Manchester, Durham University, University of Aberdeen, University of Bergen and UniResearch CIPR) are building their own digital outcrop databases. Due to the strong industry involvement, these and other databases
660 (see SAFARI [52] and FAKTS [53]) are excluded from public access. Recent developments aim at providing digital outcrops in an open-access manner [54] to resolve the issue. Furthermore, due to the vertical positioning problem above,

easy access to high- and medium resolution DEMs is important. As demonstrated by recent measurement, the usage of DEMs has a significant influence
665 on the projection accuracy of image-based interpretation on mobile device towards 3D surface models [20].

One particular challenge in digital field geology is the treatment of environmental changes. Digital outcrops are infrequently collected and the textured models are used for field study all across the year. Therefore, in image registration terms, there is a drastic difference in local illumination, moisture content
670 as well as fog and snow between acquired 3D surface models and the outcrop images collected during field trips. The issue has been previously discussed in terms of illumination differences [55], but drastic changes in terms of fog and moisture are still problematic to treat. Therefore, it is advisable to collect digital outcrop models for prominent locations in different seasonal conditions to allow for variety in model selection when planning field trips.

Currently available systems that provide digital outcrop interpretation capabilities on mobile devices in 3D include GRIT [29] and Outcrop [30], though earlier prototypes have been demonstrated [56]. Outcrop, developed by Centre
680 Européen de Recherche et d'Enseignement des Géosciences de l'Environnement (CEREGE) at Aix-Marseille Université, is a mobile device app for Android devices that is able to load and process various forms of numerical outcrops. Its major focus is the documentation of structural features (e.g. fault areas, fractures and rock deformations) on outcrops using line interpretations. Furthermore,
685 it is possible to pin extended note annotations to the model. GRIT, developed as a collaboration between UniResearch AS CIPR, University of Bergen, University of Aberdeen and CEREGE, is a mobile device app for Android devices that can handle large-area digital outcrops of tens of kilometres in surface length in 3D. Its major focus is the documentation of the sedimentary- and stratigraphic
690 architecture (e.g. strata boundaries, depositional object envelopes, facies areas) on outcrops via lines, polygons and brushes. The interpretations are mapped in a 2D-3D interplay between outcrop surface and field photograph.

[comparison photo: GRIT and Outcrop]

- recap: task to be solved
- 695 • main requirements for (location- and orientation) sensor accuracy and geometric accuracy
- specific requirements to this use case: data availability; illumination; network inavailability
- available approach to address the task

700 *6.3. Virtual Field Trips*

- recap: task to be solved
- main requirements for (location- and orientation) sensor accuracy and geometric accuracy
- specific requirements to this use case: data availability; illumination; network inavailability
- 705 • available approach to address the task

7. Conclusions

This article assessed the possibility of interactive interpretation and annotation of 3D outcrops on mobile devices in multiple geoscientific domains. Due 710 to the research effort in recent years, novel mobile applications such as Open-WaterLevels for surface hydrology and GRIT for field geology were introduced to the community to bridge the gap between lab assessment and outdoor field work for data interpretation. This article also showed further application areas that build upon mobile device technology and the interactive annotation of 3D 715 surface data for geoscientific problem solving.

McCaffery et al. proposed the use of mobile devices for field interpretation in geology in 2005 [5]. The technological specifics of mobile device app development hampered the progress on this goal for years. Only recent advancements in efficient treatment of 3D data [?], algorithmic proposals for image-to-geometry

720 registration (see [18, 20]) and on-device 3D rendering (as presented in [32] and in
this article for point-based surface) specifically designed for mobile devices make
the actual use for geoscientific applications in the field possible. The utilisation
of crowdsourced VGI and introduction of mobile devices as low-cost measuring
devices for real-world problems [57] contribute to the acceptance of this mobile
725 device technological development within the geoscientific community. Computer
Vision challenges such as image registration under changing illumination condi-
tions and with reduced image resolution can be viewed as "sufficiently solved"
to make photogrammetric- and vision-based algorithms applicable to real-world
outdoor settings, while still leaving space for improvement and quality and per-
730 formance.

The measurements found in this article as well as its related studies suggest
that localisation and orientation of mobile device sensors with respect to the
application-specific accuracy requirements is a persisting challenge. The sensors
employed by low-cost devices have accuracy limitations. Sensor filtering- and fu-
735 sion techniques are required to even moderately consider the use of such sensor
data. Environmental effects such as device-internal heating processes and the
system-internal handling of sensor initialisation further complicate the calibra-
tion of such sensors without user involvement.

Furthermore, this study gives a representative overview about the energy
740 consumption of mobile apps employing 3D surfaces, computer vision and com-
puter graphics procedures. It was shown that the distinction between 2D- and
3D data used by mobile apps significantly drives the power consumption, and
therefore the operation time of the mobile field apps during a study. Means of
reducing the power consumption in the future have, next to extended periods
745 of app use by domain experts, beneficial secondary effects: power-reduced main
functions of the mobile app allow energy-expensive simultaneous localisation
and mapping (SLAM) techniques to be used for sensor data augmentation.

Lastly, the treatment of vegetation within scanned- and photographed data
during mobile field studies remains a challenge in the context of interactive in-
750 terpretation. 3D reference data are obtained less frequent than they are used

in a given outdoor setting. Vegetation itself is visually dynamic content that complicates image registration to existing 3D data, which complicates interpretations in common outdoor settings. While current procedures of data processing try to segment- and remove vegetation data from scans [], it leaves the mobile device app less information to work with when registering photos. Therefore, proposing means of 3D topographic data processing that homogenizes vegetation in 3D scans and photos without removing the related data will have an impact on accurate outdoor photo registration on 3D base data.

8. Discussion

- 760 • porting existing desktop algorithms on mobile devices [quick and fast]
• pre-processing of geodata for mobile use

Acknowledgements

First, we would like to thank M.Sc. Richard Boerner from TU Munich, Germany for his assistance with the development of an alternative approach for 765 synthetic image generation using perspective 3D to 2D image projection with respect to object space definition and to solve for point occlusions (see section 4). Furthermore, we want graduate the European Social Fund and the Free State of Saxony for their financial support (funding no. 100235479).

References

- 770 [1] C. Wu, Towards linear-time incremental structure from motion, in: 2013 International Conference on 3D Vision - 3DV 2013, 2013, pp. 127–134.
doi:10.1109/3DV.2013.25.
- [2] M. Goesele, N. Snavely, B. Curless, H. Hoppe, S. M. Seitz, Multi-view stereo for community photo collections, in: Computer Vision, 2007. ICCV 775 2007. IEEE 11th International Conference on, IEEE, 2007, pp. 1–8.

- [3] M. Kröhnert, C. Kehl, H. Litschke, S. J. Buckley, Image-to-geometry registration on mobile devices - concepts, challenges and applications, in: L. Paul, G. Stanke, M. Pochanke (Eds.), 3D-NordOst, volume 20, Gesellschaft zur Förderung angewandter Informatik, 2017, pp. 99–108.
- 780 [4] I. Trinks, P. Clegg, K. McCaffrey, R. Jones, R. Hobbs, B. Holdsworth, N. Holliman, J. Imber, S. Waggott, R. Wilson, Mapping and analysing virtual outcrops, *Visual Geosciences* 10 (2005) 13–19.
- 785 [5] K. McCaffrey, R. Jones, R. Holdsworth, R. Wilson, P. Clegg, J. Imber, N. Holliman, I. Trinks, Unlocking the spatial dimension: digital technologies and the future of geoscience fieldwork, *Journal of the Geological Society* 162 (2005) 927–938.
- [6] S. J. Buckley, J. A. Howell, H. D. Enge, T. H. Kurz, Terrestrial laser scanning in geology: data acquisition, processing and accuracy considerations, *Journal of the Geological Society* 165 (2008) 625–638.
- 790 [7] G. Caumon, G. Gray, C. Antoine, M. O. Titeux, Three-dimensional implicit stratigraphic model building from remote sensing data on tetrahedral meshes: Theory and application to a regional model of la popa basin, ne mexico, *IEEE Transactions on Geoscience and Remote Sensing* 51 (2013) 1613–1621.
- 795 [8] E. Schwalbe, H.-G. Maas, The determination of high-resolution spatio-temporal glacier motion fields from time-lapse sequences, *Earth Surface Dynamics* 5 (2017) 861–879.
- 800 [9] P. Letortu, M. Jaud, P. Grandjean, J. Ammann, S. Costa, O. Maquaire, R. Davidson, N. L. Dantec, C. Delacourt, Examining high-resolution survey methods for monitoring cliff erosion at an operational scale, *GIScience & Remote Sensing* (2017) 1–20.
- [10] M. Medjkane, O. Maquaire, S. Costa, T. Roulland, P. Letortu, C. Fauchard, R. Antoine, R. Davidson, High-resolution monitoring of complex coastal

- 805 morphology changes: cross-efficiency of SfM and TLS-based survey (vaches-noires cliffs, normandy, france), Landslides (2018).
- [11] Y. Watanabe, Y. Kawahara, UAV photogrammetry for monitoring changes in river topography and vegetation, Procedia Engineering 154 (2016) 317–325.
- 810 [12] M. Kröhnert, R. Meichsner, Segmentation of environmental time lapse image sequences for the determination of shore lines captured by hand-held smartphone cameras, ISPRS Annals of the Photogrammetry, Remote Sensing and Spatial Information Sciences IV-2/W4 (2017) 1–8.
- 815 [13] J. G. Leskens, C. Kehl, T. Tutenel, T. Kol, G. de Haan, G. Stelling, E. Eismann, An interactive simulation and visualization tool for flood analysis usable for practitioners, Mitigation and Adaptation Strategies for Global Change (2015) 1–18.
- [14] E. N. Mueller, A. Pfister, Increasing occurrence of high-intensity rainstorm events relevant for the generation of soil erosion in a temperate lowland region in central europe, Journal of Hydrology 411 (2011) 266 – 278.
- 820 [15] S. García, R. Pagés, D. Berjón, F. Morán, Textured splat-based point clouds for rendering in handheld devices, in: Proceedings of the 20th International Conference on 3D Web Technology, Web3D ’15, ACM, New York, NY, USA, 2015, pp. 227–230. URL: <http://doi.acm.org/10.1145/2775292.2782779>.
- 825 [16] T. G. Farr, P. A. Rosen, E. Caro, R. Crippen, R. Duren, S. Hensley, M. Kobrick, M. Paller, E. Rodriguez, L. Roth, et al., The shuttle radar topography mission, Reviews of geophysics 45 (2007).
- [17] C. Kehl, S. Buckley, R. Gawthorpe, I. Viola, J. Howell, DIRECT IMAGE-TO-GEOMETRY REGISTRATION USING MOBILE SENSOR DATA, ISPRS Annals of Photogrammetry, Remote Sensing & Spatial Information Sciences 3 (2016) 121–128.

- [18] S. Gauglitz, C. Sweeney, J. Ventura, M. Turk, T. Hollerer, Model estimation and selection towards unconstrained real-time tracking and mapping, *Visualization and Computer Graphics, IEEE Transactions on* 20 (2014) 825–838.
- [19] C. Sweeney, J. Flynn, B. Nuernberger, M. Turk, T. Hollerer, Efficient computation of absolute pose for gravity-aware augmented reality, in: *Mixed and Augmented Reality (ISMAR), 2015 IEEE International Symposium on*, 2015, pp. 19–24.
- [20] C. Kehl, S. J. Buckley, S. Viseur, R. L. Gawthorpe, J. R. Mullins, J. A. Howell, Mapping field photos to textured surface meshes directly on mobile devices, *The Photogrammetric Record* 32 (2017) 398–423.
- [21] R. Boerner, M. Kröhnert, Brute force matching between camera shots and synthetic images from point clouds, volume XLI-B5, 2016, pp. 771–777. doi:[doi:10.5194/isprs-archives-XLI-B5-771-2016](https://doi.org/10.5194/isprs-archives-XLI-B5-771-2016).
- [22] P. Viola, W. M. Wells, Alignment by maximization of mutual information, *International journal of computer vision* 24 (1997) 137–154.
- [23] M. Corsini, M. Dellepiane, F. Ganovelli, R. Gherardi, A. Fusiello, R. Scopigno, Fully Automatic Registration of Image Sets on Approximate Geometry, *International journal of computer vision* 102 (2013) 91–111.
- [24] M. J. Powell, The newuoia software for unconstrained optimization without derivatives, in: *Large-scale nonlinear optimization*, Springer, 2006, pp. 255–297.
- [25] F. Ponchio, M. Dellepiane, Multiresolution and fast decompression for optimal web-based rendering, *Graphical Models* 88 (2016) 1 – 11.
- [26] J. L. Bentley, Multidimensional binary search trees used for associative searching, *Communications of the ACM* 18 (1975) 509–517.

- [27] J. Kessenich, G. Sellers, D. Shreiner, OpenGL Programming Guide: The Official Guide to Learning OpenGL, Version 4.5 with SPIR-V, OpenGL, Pearson Education, 2016. URL: <https://books.google.fr/books?id=vUK1DAAAQBAJ>.
- [28] P. Mehta, Learn OpenGL ES: For Mobile Game and Graphics Development, Apress, 2013. URL: <https://books.google.dk/books?id=Ra09AAAAQBAJ>.
- [29] C. Kehl, J. R. Mullins, S. J. Buckley, R. L. Gawthorpe, J. A. Howell, I. Viola, S. Viseur, Geological Registration and Interpretation Toolbox (GRIT): A Visual and Interactive Approach for Geological Interpretation in the Field, in: Proceedings of 2nd Virtual Geoscience Conference, 2016, pp. 59–60.
- [30] S. Viseur, R. Roudaut, R. Bertozzi, M. Castelli, J.-L. Mari, 3d interactive geological interpretations on digital outcrops using a touch pad, in: Vertical Geology Conference (VGC), 2014.
- [31] C. Kehl, S. J. Buckley, J. A. Howell, Image-to-Geometry Registration on Mobile Devices - An Algorithmic Assessment, in: Proceedings of the 3D-NordOst workshop, volume 18, GFaI, 2015, pp. 17–26. ISBN 978-3-942709-14-9.
- [32] M. Agus, E. Gobbetti, F. Marton, G. Pintore, P.-P. Vázquez, Mobile Graphics, in: A. Bousseau, D. Gutierrez (Eds.), EuroGraphics 2017 - Tutorials, The Eurographics Association, 2017. doi:10.2312/egt.20171032.
- [33] S. Heymann, K. Müller, A. Smolic, B. Froehlich, T. Wiegand, Sift implementation and optimization for general-purpose gpu, Winter School of Computer Graphics (WSCG) (2007).
- [34] M. A. Hudelist, C. Cobârzan, K. Schoeffmann, Opencv performance measurements on mobile devices, in: Proceedings of International Conference on Multimedia Retrieval, ICMR '14, ACM, New York, NY,

- USA, 2014, pp. 479:479–479:482. URL: <http://doi.acm.org/10.1145/2578726.2578798>. doi:10.1145/2578726.2578798.
- [35] D. Chait, Using ASTC Texture Compression for Game Assets, whitepaper, NVIDIA Corporation, 2015. URL: <https://developer.nvidia.com/astc-texture-compression-for-game-assets>.
- [36] S. Siedschlag, Wasserstände und Durchflüsse - messen, speichern und übertragen im digitalen Zeitalter, in: Dresdner Wasserbauliche Mitteilungen, volume 53 of *Dresdner Wasserbauliche Mitteilungen*, Technische Universität Dresden, Institut für Wasserbau und technische Hydromechanik, 2015. URL: <https://henry.baw.de/handle/20.500.11970/103357>.
- [37] I. Horner, B. Renard, J. L. Coz, F. Branger, H. McMillan, G. Pierrefeu, Impact of stage measurement errors on streamflow uncertainty, Water Resources Research (2018).
- [38] Saxon Flood Centre, Water levels & flow rates, 2018. URL: <https://www.umwelt.sachsen.de/umweltinfosysteme/hwims/portal/web/wasserstand-uebersicht>, accessed: 2018-03-05.
- [39] U. Büttner, E. Wolf, Konzeption des gewässerkundlichen pegelnetzes in sachsen, 38. Dresdner Wasserbaukolloquium 2015 Messen und Überwachen im Wasserbau und am Gewässer (2015).
- [40] S. Etter, B. Strobl, Crowdwater, 2018. URL: <http://www.crowdwater.ch/de/home/>, accessed: 2018-03-06.
- [41] Kisters, Einfach smart: App für Pegelmessung auf Knopfdruck, 2014. URL: https://www.kisters.de/fileadmin/user_upload/Wasser/Produkte/WISKI/Produktblaetter/MobileWaterTracker_de_mail.pdf, accessed: 2018-03-06.
- [42] M. Harman, Open Camera - Camera app for Android, 2017. URL: <https://sourceforge.net/projects/opencamera/>, version 1.38.

- [43] J. R. Blum, D. G. Greencorn, J. R. Cooperstock, Smartphone sensor reliability for augmented reality applications, in: K. Zheng, M. Li, H. Jiang (Eds.), *Mobile and Ubiquitous Systems: Computing, Networking, and Services*, Springer Berlin Heidelberg, Berlin, Heidelberg, 2013, pp. 233 – 248.
- [44] C. Bauer, On the (in-)accuracy of gps measures of smartphones: A study of running tracking applications, in: *Proceedings of International Conference on Advances in Mobile Computing & Multimedia*, MoMM '13, ACM, New York, NY, USA, 2013, pp. 335:335–335:341. URL: <http://doi.acm.org/10.1145/2536853.2536893>. doi:10.1145/2536853.2536893.
- [45] P. A. Zandbergen, S. J. Barbeau, Positional accuracy of assisted GPS data from high-sensitivity GPS-enabled mobile phones, *Journal of Navigation* 64 (2011) 381–399.
- [46] S. K. Moore, Superaccurate gps coming to smartphones in 2018, *IEEE Spectrum* (2017). Accessed: 2018-03-06.
- [47] G. Liu, K. M. A. Hossain, M. Iwai, M. Ito, Y. Tobe, K. Sezaki, D. Matekenya, Beyond horizontal location context: measuring elevation using smartphone's barometer, in: *Proceedings of the 2014 ACM International Joint Conference on Pervasive and Ubiquitous Computing Adjunct Publication*, ACM Press, 2014. doi:10.1145/2638728.2641670.
- [48] S. J. Buckley, E. Schwarz, V. Terlaky, J. A. Howell, R. Arnott, Combining Aerial Photogrammetry and Terrestrial Lidar for Reservoir Analog Modeling, *Photogrammetric Engineering & Remote Sensing* 76 (2010) 953–963.
- [49] T. J. Dewez, J. Leroux, S. Morelli, Uav sensing of coastal cliff topography for rock fall hazard applications, in: *Journées Aléas Gravitaires JAG 2015*, 2015.
- [50] J. Chandler, S. Buckley, Structure from motion (SFM) photogrammetry vs terrestrial laser scanning, American Geosciences Institute (AGS), 2016.

- 940 [51] C. Kehl, J. R. Mullins, S. J. Buckley, J. A. Howell, R. L. Gawthorpe,
Interpretation and mapping of geological features using mobile devices in
outcrop geology - a case study of the saltwick formation, north yorkshire,
uk, AGU Books - Special Issue (2018 (accepted for publication)).
- 945 [52] T. Dreyer, L.-M. Fält, T. Høy, R. Knarud, J.-L. Cuevas, et al., Sedimentary
architecture of field analogues for reservoir information (SAFARI): a
case study of the fluvial escanilla formation, spanish pyrenees, in: The
Geological Modeling of Hydrocarbon Reservoirs and Outcrop Analogs,
volume 15, International Association of Sedimentologists – Special Pub-
lications, Wiley Online Library, 1993, pp. 57–80.
- 950 [53] L. Colombera, F. Felletti, N. P. Mountney, W. D. McCaffrey, A data-
base approach for constraining stochastic simulations of the sedimentary
heterogeneity of fluvial reservoirs, AAPG bulletin 96 (2012) 2143–2166.
- 955 [54] A. J. Cawood, C. E. Bond, erock: an online, open-access repository of vir-
tual outcrops and geological samples in 3d, in: EGU Geophysical Research
Abstracts, volume 20, 2018, p. 18248.
- [55] C. Kehl, S. J. Buckley, S. Viseur, R. L. Gawthorpe, J. A. Howell, Automatic
illumination-invariant image-to-geometry registration in outdoor environ-
ments, The Photogrammetric Record 32 (2017) 93–118.
- 960 [56] L. Hama, R. A. Ruddle, D. Paton, 3d mobile visualization techniques in
field geology interpretation: Evaluation of modern tablet applications, in:
AAPG Hedberg Research Conference: 3D Structural Geologic Interpreta-
tion: Earth, Mind and Machine, 2013.
- 965 [57] A. Eltner, H. Sardemann, M. Kröhnert, E. Schwalbe, Camera based low-
cost system to monitor hydrological parameters in small catchments, in:
EGU General Assembly Conference Abstracts, volume 19, 2017, p. 6698.

Highlights

- point 1
- point 2
- 970 • point 3
- point 4
- point 5